

Atomistic spin-orbit coupling and $\mathbf{k}\cdot\mathbf{p}$ parameters in III-V semiconductors

J.-M. Jancu,¹ R. Scholz,² E. A. de Andrada e Silva,³ and G. C. La Rocca⁴

¹*Laboratoire de Photonique et de Nanostructures, CNRS, route de Nozay, F-91000 Marcoussis, France*

²*Institut für Physik, Technische Universität Chemnitz, D-09107 Chemnitz, Germany*

³*Instituto Nacional de Pesquisas Espaciais, C.P. 515, 12201-970 São José dos Campos - SP, Brazil*

⁴*Scuola Normale Superiore and L'Istituto Nazionale per la Fisica della Materia, Piazza dei Cavalieri 7, I-56126 Pisa, Italy*

(Received 10 August 2005; published 2 November 2005)

The most accurate description of spin splittings in semiconductor nanostructures has been obtained from a 14-band $\mathbf{k}\cdot\mathbf{p}$ model, but the historical way in which it has developed from the 8-band Kane model has endorsed somewhat arbitrary values of the momentum and spin-orbit matrix elements. We have systematically determined the 14-band $\mathbf{k}\cdot\mathbf{p}$ parameters for III-V semiconductors from a 40-band tight-binding model. Significant changes with respect to previously accepted values were found even for GaAs. For all materials investigated, the resulting Dresselhaus spin-orbit coupling parameter is in good agreement with experimental values. The atomistic background of the present parametrization allows new insight into the spin-orbit coupling Δ^- between bonding and antibonding orbitals and its dependence on ionicity.

DOI: [10.1103/PhysRevB.72.193201](https://doi.org/10.1103/PhysRevB.72.193201)

PACS number(s): 71.70.Ej, 71.15.Ap, 73.21.Fg, 85.75.-d

The great technological importance of III-V semiconductor compounds derives from their electronic structure near the band gap. For this reason, the multiband $\mathbf{k}\cdot\mathbf{p}$ Kane model¹ had a major impact in the development of semiconductor physics and their applications. More recently, there has been a strong revival of the interest in spin effects in semiconductors, stimulated by the goal of developing a new generation of electronic devices based on the control of the carrier spin besides their electric charge.^{2,3} The bulk inversion asymmetry (BIA) in the III-V semiconductors results in a lifting of spin degeneracy in the conduction band, proportional to the third power of the wave vector near the center of the Brillouin zone, $\delta = \gamma_c k$.^{3,4} γ_c is called Dresselhaus spin-orbit (SO) coupling parameter and its exact value is essential for a detailed understanding of spin dynamics and for the design of spintronic devices, in particular those that depend on the interference between the BIA (or Dresselhaus) and SIA (structural inversion asymmetry, or Rashba) spin-orbit terms.⁵⁻⁷ The BIA spin splitting in the conduction band has been investigated both experimentally⁸⁻¹² and theoretically,¹²⁻¹⁴ however, for most III-V compounds, γ_c is still not well known. In particular for InAs, one of the most promising semiconductor materials for spintronic applications, an early estimate for γ_c (Ref. 15) has been used in different calculations,^{7,15-18} but recent predictions resulted in a much lower value.³ As a matter of fact, there is a strong need for a systematic and reliable determination of asymmetry-related parameters in several bulk semiconductors and their heterostructures.

Most calculations of quantum devices are based on the $\mathbf{k}\cdot\mathbf{p}$ method and its generalization in terms of the envelope-function approximation,^{19,20} and many quantities can be derived even from simplified versions of this theory, such as the single band effective-mass model. While a meaningful description of the Rashba spin splitting due to a mesoscopic structural asymmetry can be obtained already in the 8-band Kane model,^{15,21} at least a 14-band $\mathbf{k}\cdot\mathbf{p}$ Hamiltonian is required to address the BIA SO coupling effects in the conduction band, as first demonstrated by Hermann and Weisbuch.²²

Later on, this 14-band model was completed by the inclusion of all the $\mathbf{k}\cdot\mathbf{p}$ interactions between the Γ_8^v and Γ_7^v valence maxima and the Γ_6^c , Γ_7^c , and Γ_8^c conduction bands,^{12-14,23} including the contributions of remote bands up to quadratic order in k . This improvement of previous $\mathbf{k}\cdot\mathbf{p}$ models involves several additional parameters that were determined in a rather nonsystematic way by fitting various measurements, or by using semiempirical rules and perturbative approaches.¹³

Conversely, recent progress enabled atomistic methods to become competitive with $\mathbf{k}\cdot\mathbf{p}$ based approaches, allowing us to calculate precise band structures of semiconductor bulk materials and their nanostructures. In particular, the extended-basis $sp^3d^5s^*$ empirical tight-binding (TB) method²⁴ has proved its ability to provide a fair view of the entire Brillouin zone, including even small details of the band structure such as spin splittings.²⁵ The interband dipole moments are calculated within the independent particle approximation using a Peierls-coupling TB scheme,²⁶ so that this 40-band TB Hamiltonian adequately reproduces band parameters, chemical trends, as well as the optical response of III-V semiconductors. This Hamiltonian contains 29 independent parameters for each bulk material, but in strong contrast with $\mathbf{k}\cdot\mathbf{p}$ theory, the strategy for their empirical determination relies on a fit of the electronic band structure over the entire Brillouin zone, with clear chemical trends between compounds sharing a group-III or group-V element. The accurate original parametrization²⁴ has been optimized further in order to obtain an improved agreement with more recent experimental data.²⁷ Here, we use the TB band structure of III-V semiconductors as an input, and in the usual subset of 14 states at Γ we determine the corresponding $\mathbf{k}\cdot\mathbf{p}$ parameters from an expansion of the TB Hamiltonian in powers of the wave vector. Our results suggest that accepted values of asymmetry-related momentum and spin-orbit matrix elements must be revised significantly, even in the reference case of GaAs.

The comparison of GaAs band structures obtained with the TB Hamiltonian and with the 14-band $\mathbf{k}\cdot\mathbf{p}$ model (using

TABLE I. $\mathbf{k}\cdot\mathbf{p}$ parameters, with dipole matrix elements and spin-orbit splittings in the notation of Fig. 1.

	AlP	GaP	InP	AlAs	GaAs	InAs	AlSb	GaSb	InSb
E_0 (eV)	3.63	2.895	1.423	3.130	1.519	0.418	2.38	0.81	0.235
E_0' (eV)	4.78	4.38	4.78	4.55	4.54	4.48	3.53	3.11	3.18
Δ_0 (eV)	0.06	0.08	0.107	0.3	0.341	0.38	0.67	0.76	0.81
Δ_0' (eV)	0.04	0.09	0.19	0.15	0.2	0.31	0.24	0.33	0.46
Δ^- (eV)	-0.03	+0.04	+0.11	-0.19	-0.17	-0.05	-0.41	-0.4	-0.26
P (eV Å)	9.51	9.53	8.45	8.88	9.88	9.01	8.57	9.69	9.63
P' (eV Å)	0.19	0.36	0.34	0.34	0.41	0.66	0.51	1.34	1.2
Q (eV Å)	8.10	8.49	7.88	8.07	8.68	7.72	7.8	8.25	7.83
C (1)	-1.36	-1.77	-1.33	-1.07	-1.76	-0.85	-0.72	-1.7	-1.19

the parameters given in Table I) are shown in Fig. 1 together with the relevant matrix elements. It is important to distinguish matrix elements allowed in the centrosymmetric limit (quasi-Ge model), i.e., P , Q , Δ_0 , and Δ_0' , from those associated with the asymmetry between anion and cation in III-V compounds, P' and Δ^- . The former show only a weak dependence on the ionicity, whereas the latter depend crucially on it. In the vicinity of the zone center, the two models for the electronic band structure agree fairly well. In particular, the valence bands and the Γ_6^c conduction band are very well fitted over a large portion of the Brillouin zone, covering energies up to about 0.5 eV around the band edge. We should point out that the corresponding Luttinger parameters, not listed in Table I because they are not relevant for the present study, are in excellent agreement with other published results.²⁷

The main discrepancy is related to the dispersion of the upper conduction bands Γ_7^c and Γ_{8c} , a problem which could be eliminated by adding the interactions of $\Gamma_{7c,8c}$ with the next higher bands in the $\mathbf{k}\cdot\mathbf{p}$ Hamiltonian, but this would go beyond the framework of the standard 14-band $\mathbf{k}\cdot\mathbf{p}$ model.^{12-14,23} As we shall prove below, the poor representation of the Γ_7^c and Γ_8^c dispersions does not significantly affect the calculation of the spin splitting around Γ_6^c . Due to the off-diagonal spin-orbit coupling Δ^- (Ref. 13), the diagonal

elements of the 14-band $\mathbf{k}\cdot\mathbf{p}$ Hamiltonian do not correspond to the eigenvalues for Γ_7^u , Γ_8^u , Γ_7^c , and Γ_8^c , so that both the $\mathbf{k}\cdot\mathbf{p}$ and TB Hamiltonians have to be defined in the basis of eigenfunctions at Γ without spin-orbit interactions. In this way, the $\mathbf{k}\cdot\mathbf{p}$ expansion and the underlying TB model describe the region around the center of the Brillouin zone with the same precision, at the expense of a poor fitting of the band structure at large wave vector. This strategy is opposite to parametrizations involving a simultaneous fitting of the band extrema at Γ , L , and X .^{28,29}

The couplings between the 14 bands visualized in Fig. 1 are treated explicitly with the formalism developed by Pfeffer and Zawadzki,²³ including the influence of remote bands on the states surrounding the gap perturbatively up to second order in k , in accordance with the definition of the Hermann-Weisbuch parameter C for the reduced mass m^* of the electrons in the Γ_6^c conduction minimum.²² The resulting $\mathbf{k}\cdot\mathbf{p}$ parameters are listed in Table I. We use the convention of Cardona *et al.*¹³ for the coordinate system with the anion at the origin and the cation at $(a/4)(111)$, involving a positive sign of all transition dipole moments.

For all the semiconductors considered, Table I demonstrates that the momentum matrix elements P and Q are in the same range as typical values used in previous $\mathbf{k}\cdot\mathbf{p}$ models. However, large differences for P' and Δ^- are observed as compared to previous estimates.^{3,12-14,23} It should be noted that the linear muffin-tin orbital (LMTO) calculations of Ref. 13 involve a specific technique for the adjustment of the unavoidable gap inaccuracies in density functional calculations, resulting in questionable estimates for the matrix elements required in $\mathbf{k}\cdot\mathbf{p}$ models. In the case of GaAs, previous values of Δ^- vary in the range from -0.05 eV (Ref. 14) to -0.11 eV (Ref. 13), in sharp contrast to the present result of -0.17 eV. The chemical trends for Δ^- observed in our calculations result from (and are consistent with) the different ionicities of III-V semiconductors and the associated asymmetric charge distribution along the bonds. The off-diagonal spin-orbit coupling Δ^- can be related to the atomic splittings Δ_a for the anion and Δ_c for the cation. Generalizing the formulae used earlier¹³ to include the empty d states, we obtain $\Gamma_4^{v,c} = \alpha_{v,c}|p_a\rangle + \beta_{v,c}|p_c\rangle + \gamma_{v,c}|d_a\rangle + \delta_{v,c}|d_c\rangle$, where the coefficients of the p -symmetric contributions are reduced due to the admixture of atomic d states, in agreement with

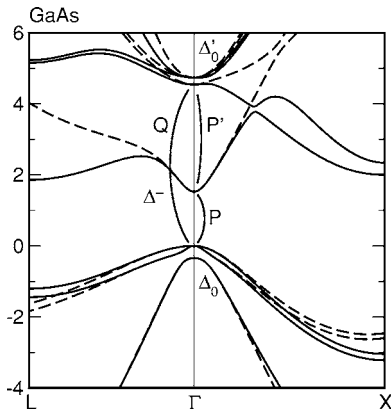


FIG. 1. Band structure of cubic GaAs as calculated with the 40-band TB model (solid lines) and the 14×14 $\mathbf{k}\cdot\mathbf{p}$ model with the parameters according to Table I (dashed lines).

TABLE II. Calculated conduction band parameters as compared to experimental results: m^* (in units of m_0), g^* , and γ_c ($\text{eV } \text{\AA}^3$), together with the contributions to γ_c according to Eqs. (2) and (3) models.

		AIP	GaP	InP	AlAs	GaAs	InAs	AlSb	GaSb	InSb
m^*	exp	-	-	0.079	-	0.067	0.023	-	0.041	0.014
	TB	0.17	0.14	0.08	0.16	0.067	0.023	0.12	0.041	0.014
	$\mathbf{k} \cdot \mathbf{p}$	0.16	0.13	0.079	0.16	0.067	0.024	0.13	0.041	0.014
g^*	exp	-	+1.90	+1.26	+1.52	-0.44	-14.9	+0.84	-9.2	-51.6
	TB	+1.92	+1.84	+1.24	+1.66	-0.11	-14.7	+0.52	-8.5	-51.9
	$\mathbf{k} \cdot \mathbf{p}$	+1.92	+1.86	+1.36	+1.56	-0.11	-14.3	+0.58	-8.5	-51.6
γ_c	exp	-	-	$\pm(7.3-9.5)^a$	-	17.4-26 ^b	-	-	$\pm 185^b$	+226 ^c
	TB	+1.9	-1.4	-8.6	+10.6	+23.6	+42.3	39.3	+168	+389
	$\mathbf{k} \cdot \mathbf{p}$	+2.1	-2.4	-10.1	+11.4	+23.7	+40.5	+40.9	+167	+326
$\gamma_c^{(0)}$	Eq. (2)	0.2	0.7	0.8	1.1	2.4	18.5	5.9	42	139
$\gamma_c^{(1)}$	Eq. (3)	1.9	-3.2	-11.1	+10.2	22	30.1	35.2	134	326

^aRef. 10.

^bRef. 12.

^cRefs. 9 and 11.

first-principle calculations.³⁰ As a consequence, the spin-orbit coupling parameter $\Delta^- = \alpha_v \alpha_c \Delta_a + \beta_v \beta_c \Delta_c$ follows approximately the difference $\Delta_a - \Delta_c$. This results in a sign reversal in the case of GaP and InP, as compared, e.g., to the arsenides.¹³

Table II lists theoretical and experimental parameters related to the lowest conduction band in III-V semiconductors. The parameter C , describing the influence of remote bands on the reduced mass m^* in the conduction band, has been discussed extensively.^{13,22,23,31} Its TB value results from the coupling between the Γ_6^c conduction minimum and the empty d and s^* bands at higher energy, and for GaAs, our calculation agrees very well with the corresponding parameter extracted from magneto-Raman experiments ($C \approx -1.7$).³² In addition, within an $sp^3d^5s^*$ TB model, the influence C' of these bands on the effective Landé factor g^* is approximately proportional to $C\Delta_d/(E_c - E_d)$, where Δ_d is the spin-orbit splitting of the d -symmetric conduction bands, resulting in values of the order of -0.03 . The effective Landé factor of the Γ_6^c electron is obtained from a prescription introduced by Roth³³

$$g^* = g_0 \left(1 - \frac{i}{m_0} \sum_{n=0}^{\infty} \frac{\langle \Gamma_{6c,\uparrow} | \hat{p}_x | u_n \rangle \langle u_n | \hat{p}_y | \Gamma_{6c,\uparrow} \rangle}{E_c - E_n} - \frac{\langle \Gamma_{6c,\uparrow} | \hat{p}_y | u_n \rangle \langle u_n | \hat{p}_x | \Gamma_{6c,\uparrow} \rangle}{E_c - E_n} \right), \quad (1)$$

where $g_0 = 2.0023$ is the Landé factor of a free electron and the summation is carried out over all Γ states, excluding the lowest conduction band. Good agreement with experimental data is observed, and the remaining deviations are inherent to the approximations involved in the model calculations.³⁴ m^* and γ_c are found by fitting the band dispersion in the range $|\mathbf{k}| < 0.01 \text{ \AA}^{-1}$ to a suitable polynomial. As expected, the 40-band TB model and the $14 \times 14 \mathbf{k} \cdot \mathbf{p}$ Hamiltonian, including the influence C of the remote conduction bands, give similar

results for m^* , where minor deviations are related to the fitting procedure defined above. The positive sign of γ_c is associated with a state of X_4 symmetry above its partner state X_3 .¹³ For GaAs, the present calculation gives $\gamma_c = 23.6 \text{ eV } \text{\AA}$, corroborated by experimental data. Small differences in the γ_c values in Table II stem from invariants of fifth order in the components of k included in the TB Hamiltonian. The two theoretical results agree with the magnitude of the experimental γ_c values found so far, except for InSb where the calculations differ from the experimental value by a factor 1.4, a discrepancy smaller than observed earlier.^{3,13,15}

The spin splitting along the (110) direction $\Gamma \rightarrow \Sigma$ is shown in Fig. 2, where the results of the TB and $\mathbf{k} \cdot \mathbf{p}$ models are superimposed. It should be noted that the splitting between the two spin orientations near the Γ point is proportional to $\gamma_c k^3$ to leading order, whereas at larger energies, higher order terms and the nonparabolicity of the conduction

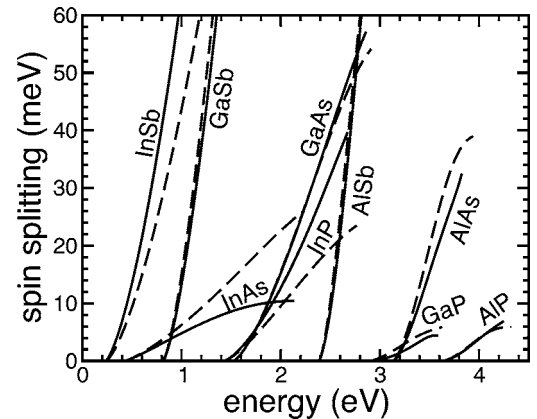


FIG. 2. Calculated zero-field spin splitting between the two spin states of the electrons, along the (110) direction $\Gamma \rightarrow \Sigma$. The spin splittings are reported as a function of the average energy of both spin states for the $sp^3d^5s^*$ TB model (solid lines), and the $14 \times 14 \mathbf{k} \cdot \mathbf{p}$ model (dashed lines).

band obscure the expected $(E-E_0)^{3/2}$ dependence. In the region of interest for experimental investigations, i.e., within about 0.3 eV above the conduction band edge, both band structure models result in excellent agreement for the spin splittings, but at higher energies, the smaller number of symmetry-adapted invariants and band states in the $\mathbf{k}\cdot\mathbf{p}$ model results in substantial deviations. This is clearly observed for semiconductors containing indium where the conduction band splitting depends strongly on the admixture between the p -symmetric valence states and empty d bands which are only 7–11 eV above the valence band maximum. For materials with the same anion, γ_c increases with the size of the cation. This trend can be assigned to a cubic term found in a third-order perturbation expansion within a 14×14 $\mathbf{k}\cdot\mathbf{p}$ Hamiltonian excluding far-level contributions. Using $\gamma_c = \gamma_c^{(0)} + \gamma_c^{(1)}$, one finds²³

$$\gamma_c^{(0)} = \frac{4}{3} P' Q P \frac{E_0 E_1 - G_0 G_1}{E_0 E_1 G_0 G_1}, \quad (2)$$

$$\gamma_c^{(1)} = -\frac{4}{9} \Delta^- Q \frac{P^2(2G_1 + E_1) - P'^2(2E'_0 + G_0)}{E_0 E_1 G_0 G_1}, \quad (3)$$

with the abbreviations $E_1 = E'_0 - E_0$, $G_0 = E_0 + \Delta_0$, and $G_1 = E_1 + \Delta'_0$. As can be deduced from Table II, γ_c is governed by $\gamma_c^{(1)}$ and the underlying value for Δ^- , revealing that a 14×14 $\mathbf{k}\cdot\mathbf{p}$ Hamiltonian is indeed the minimum framework for a reliable calculation of γ_c . It should be noted that our results are in sharp contrast with previous calculations^{13,23}

where $\gamma_c^{(1)}$ is found to contribute only about one-third to γ_c .

In addition to the above discussion of bulk properties, Stadele *et al.*³⁵ have demonstrated that the $sp^3d^5s^*$ TB model compares well with the measured nonparabolicity and warping of the conduction band in thin GaAs quantum wells, whereas previous $\mathbf{k}\cdot\mathbf{p}$ parametrizations resulted in some deviations. From the nice agreement between our new $\mathbf{k}\cdot\mathbf{p}$ parametrization and the underlying TB model, we expect an excellent transferability of the bulk $\mathbf{k}\cdot\mathbf{p}$ parameters to calculations of heterostructures in the envelope function approximation.

In conclusion, we have demonstrated that a 14-band $\mathbf{k}\cdot\mathbf{p}$ Hamiltonian implemented in the context of a precise tight-binding parametrization captures most atomistic details of the chemical and environmental effects together with the resulting spin splittings. Even though these phenomena were not considered in previous $\mathbf{k}\cdot\mathbf{p}$ parametrizations, the present work reveals their crucial importance for modeling the asymmetry-induced spin splitting of the conduction band. We expect that this new $\mathbf{k}\cdot\mathbf{p}$ parametrization also provides a valid framework for the calculation of spin-related phenomena in quantum heterostructures, an important prerequisite for a reliable modeling of semiconductor spintronic devices. Clearly, measurements of the BIA spin splitting in bulk InAs would be a drastic check of the present results.

The authors thank P. Voisin and F. Bassani for clarifying discussions and a critical reading of the manuscript.

-
- ¹E. O. Kane, *J. Phys. Chem. Solids* **1**, 249 (1957).
²I. Žutić *et al.*, *Rev. Mod. Phys.* **76**, 323 (2004).
³R. Winkler, *Spin-Orbit Coupling Effects in Two-Dimensional Electron and Hole Systems* (Springer, Berlin, 2003), p. 74.
⁴G. Dresselhaus, *Phys. Rev.* **100**, 580 (1955).
⁵S. D. Ganichev *et al.*, *Nature* **417**, 153 (2002).
⁶J. Schliemann *et al.*, *Phys. Rev. Lett.* **90**, 146801 (2003).
⁷R. de Sousa and S. Das Sarma, *Phys. Rev. B* **68**, 155330 (2003).
⁸Y.-F. Chen *et al.*, *Phys. Rev. B* **32**, 890 (1985).
⁹S. Gopalan *et al.*, *Phys. Rev. B* **32**, 903 (1985).
¹⁰A. T. Gorelenok *et al.*, *Sov. Phys. Semicond.* **20**, 216 (1986).
¹¹M. Cardona *et al.*, *Solid State Commun.* **60**, 17 (1986).
¹²G. E. Pikus *et al.*, *Sov. Phys. Semicond.* **22**, 115 (1988).
¹³M. Cardona *et al.*, *Phys. Rev. B* **38**, 1806 (1988).
¹⁴H. Mayer and U. Rössler, *Phys. Rev. B* **44**, 9048 (1991).
¹⁵E. A. de Andrada e Silva *et al.*, *Phys. Rev. B* **50**, 8523 (1994).
¹⁶A. Lusakowski *et al.*, *Phys. Rev. B* **68**, 081201(R) (2003).
¹⁷V. I. Perel' *et al.*, *Phys. Rev. B* **67**, 201304(R) (2003).
¹⁸C. L. Romano *et al.*, *Phys. Rev. B* **71**, 035336 (2005).
¹⁹G. Bastard *et al.*, in *Solid State Physics*, edited by H. Ehrenreich and D. Turnbull (Academic, Boston, 1991), Vol. 44, p. 229.
²⁰D. L. Smith and C. Mailhot, *Rev. Mod. Phys.* **62**, 173 (1990).
²¹E. A. de Andrada e Silva *et al.*, *Phys. Rev. B* **55**, 16293 (1997).
²²C. Hermann and C. Weisbuch, *Phys. Rev. B* **15**, 823 (1977).
²³P. Pfeffer and W. Zawadzki, *Phys. Rev. B* **53**, 12813 (1996).
²⁴J.-M. Jancu *et al.*, *Phys. Rev. B* **57**, 6493 (1998).
²⁵J.-M. Jancu *et al.*, *Phys. Rev. B* **70**, 121306(R) (2004).
²⁶T. B. Boykin and P. Vogl, *Phys. Rev. B* **65**, 035202 (2002).
²⁷I. Vurgaftman *et al.*, *J. Appl. Phys.* **89**, 5815 (2001).
²⁸M. Cardona and F. Pollak, *Phys. Rev.* **142**, 530 (1966).
²⁹S. Richard *et al.*, *Phys. Rev. B* **70**, 235204 (2004).
³⁰P. Boguslawsky and I. Gorczyca, *Semicond. Sci. Technol.* **9**, 2169 (1994).
³¹T. E. Ostromek, *Phys. Rev. B* **54**, 14467 (1996).
³²G. Ambrazevicius *et al.*, *Phys. Rev. Lett.* **59**, 700 (1987).
³³L. M. Roth *et al.*, *Phys. Rev.* **114**, 90 (1959).
³⁴M. Oestreich and W. W. Rühle, *Phys. Rev. Lett.* **74**, 2315 (1995).
³⁵M. Stadele *et al.*, *J. Appl. Phys.* **91**, 9435 (2002).